Mesoscopic Fano Effect through a Quantum Dot in an Aharonov-Bohm Ring

Kensuke Kobayashi [a,1] Hisashi Aikawa [a], Shingo Katsumoto [a], and Yasuhiro Iye [a]

[a] *Institute for Solid State Physics, University of Tokyo, 5-1-5 Kashiwanoha, Chiba 277-8581, Japan*

Abstract

The Fano effect illustrates how the interference and resonance cooperatively occur between a discrete state and a continuum energy state. We have realized a tunable Fano system by fabricating a quantum dot embedded in an Aharonov-Bohm ring on a 2DEG. In the Coulomb oscillation, clear asymmetric lineshapes were observed, which manifest the formation of the Fano state, namely, a mixture of the discrete state and the continuum state. The non-equilibrium transport and the temperature dependence reveal the essential role of the coherence for this effect. Through the phase controlling by the magnetic flux piercing the ring, Fano's asymmetric parameter q is obtained as a complex number for the first time.

Key words: Quantum Dot, Aharonov-Bohm Ring, Fano Effect, Coherence
PACS: 73.21.La, 85.35.-p, 73.23.Hk, 72.15.Qm

1. Introduction

An Aharonov-Bohm (AB) ring and a quantum dot (QD) are typical complementary mesoscopic systems: the wave nature of electron manifests itself in the former while the particle nature of electron features in the latter. A combination of these two into a hybrid one, therefore, enables us to explore the problem how coherent is the transport of electrons through a QD, where many electrons interact with each other. In 1995, Yacoby *et al.* [1] performed a pioneering work to address this issue by using such a system, namely a QD embedded in one arm of an AB ring. It was found [1,2] that an electron at least partially maintains its coherence in passing a QD and each level inside the QD acts as a Breit-Wigner type scatterer. In these experiments, however, the transport properties of a QD have been the main scope and the other arm with no QD has served as "reference". Here, one might ask what happens if the coherence of the QD-AB-ring hybrid system is fully maintained and thus the arm as well as the QD should be equally treated. In this situation, the Fano effect is expected to occur [3–9].

The Fano effect emerges in a system where a discrete state and the continuum energy state coexist [10]. The essence lies in the quantum interference between the two configurations in the transition process into the final states with the same energy as sketched in Fig. 1 (a); one directly through the continuum and the other through the resonance level arising around the discrete state. This "configuration interaction" yields the peculiar asymmetric lineshape in the transition probability P as a function of energy ϵ given by

[1] Corresponding author. E-mail: knsk@issp.u-tokyo.ac.jp

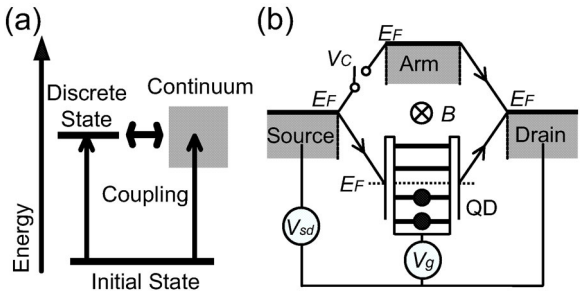

Fig. 1. (a) Principle of the Fano effect. (b) Schematic representation of the present tunable Fano system. The position of the single-particle levels inside the QD is controlled by V_g, the coupling between the continuum and the discrete levels by V_C, and the phase difference between two paths by B penetrating the ring.

$$P(\tilde{\epsilon}) \propto \frac{(\tilde{\epsilon}+q)^2}{\tilde{\epsilon}^2+1}, \quad \tilde{\epsilon} = \frac{\epsilon-\epsilon_0}{\Gamma/2}, \tag{1}$$

where ϵ_0 is the energy level of the resonance state and Γ is its width. The parameter q, which is the ratio of the matrix elements linking the initial state to the discrete and continuum parts of the final state, serves as a measure of the degree of coupling between both. Since in the original Fano model no extra phase is attached to an electron when it goes in and out from the discrete state, q is usually treated as a real parameter.

Since its establishment in the atomic physics more than 40 years ago, this effect has been ubiquitously found in a large variety of experiments [11–13]. As it is essentially a single-impurity problem, an observation on a single site, for example in the electron transport, would reveal Fano physics in a more transparent way. Compared to its long history in the spectroscopy, however, its general importance in the transport was only recently pointed out [14,15]. Experimentally, the single-site Fano effect has been reported in the scanning tunneling spectroscopy of an atom on the surface [16,17] and in transport through a QD [18,19]. While the latter case is the first observation of this effect in a mesoscopic system, the mechanism that makes it bring about is not clarified. In this sense, as has been proved [20], a QD-AB-ring hybrid system serves as a well-defined Fano system where the transition process shown in Fig. 1 (a) is realized in the real space as sketched in Fig. 1 (b). An electron traverses from the source to the drain along two interfering paths. One is through the discrete state in the QD and the other through the arm.

Here, by using a Fano system, we clarify characteristic transport arising from this effect, such as the delocalization of the discrete level and the unique temperature dependence. Magnetic field control of the relative phase between the discrete state and the continuum indicates that Fano's parameter q should be extended to be complex rather than real and the complex q is actually obtained.

2. Experiment

Figure 2 shows the fabricated Fano system on a two-dimensional electron gas (2DEG) system at an AlGaAs/GaAs heterostructure (mobility $= 9 \times 10^5$ cm^2/Vs and sheet carrier density $= 3.8 \times 10^{11}$ cm^{-2}). The ring-shaped conductive region was formed by wet-etching the 2DEG. The white regions indicate the Au/Ti metallic gates deposited to control the device. A QD can be defined in the lower arm by applying the side-gate voltages (V_L and V_R). As sketched in Fig. 1 (b), the present system is characterized by its controllability. The single-particle level of the QD can be tuned by V_g. The gate in the upper arm (V_C) is for switching the transition through the continuum state on and off. The magnetic field (B) penetrating the ring can control the phase difference between the two paths. Measurements were performed in a dilution refrigerator by a standard lock-in technique in the two-terminal setup with an excitation voltage of 10 μV (80 Hz) between the source and the drain.

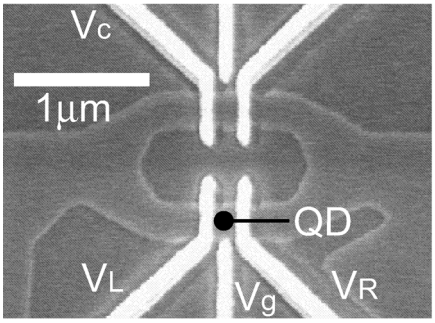

Fig. 2. Scanning electron micrograph of the correspondent device.

3. Results and Discussion

3.1. *Fano Effect in the Coulomb Oscillation*

First we pinched off the upper arm by applying large negative voltage on V_C. The QD was defined in the lower arm by tuning the side-gate voltages (V_L and V_R). The lower panel of Fig. 3 (a) shows the pronounced peaks in the conductance through the QD as sweeping V_g, namely, a typical Coulomb oscillation expected for QD's in the Coulomb blockade (CB) regime. The small irregularity of the peak positions reflects that of the addition energy and supports the occurrence of transport through each single level inside the QD.

Next, we made the upper arm conductive. Because the control gate and the QD are well separated electrostatically, a clear one-to-one correspondence is observed between the two results in Fig. 3 (a), ensuring that the discreteness of the energy levels in the QD is maintained. It is noteworthy that the line shapes of the oscillation become very asymmetric and show even dip structures. The asymmetric line shape observed above is a clear sign of the Fano effect.

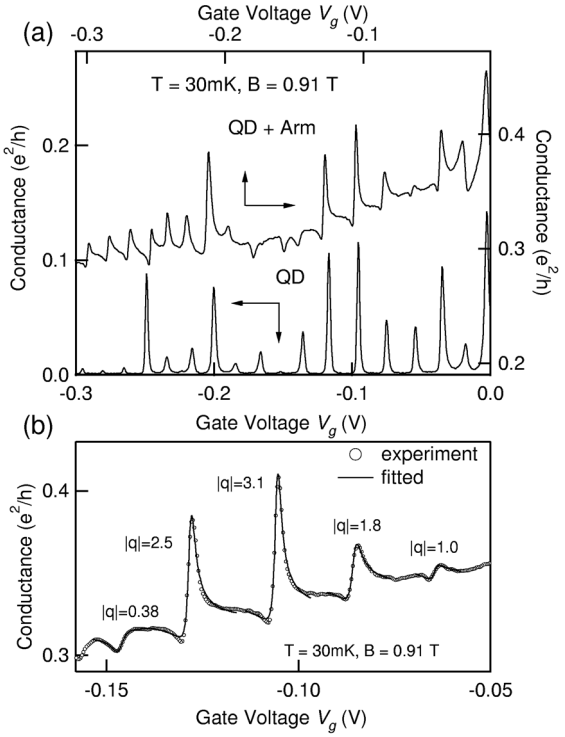

Fig. 3. (a) Typical Coulomb oscillation at $V_C = -0.12$ V with the arm pinched off, and asymmetric Coulomb oscillation at $V_C = -0.086$ V with the arm transmissible. The latter shows a clear Fano effect. Both of them were obtained at $T = 30$ mK and $B = 0.91$ T. (b) Typical results of the fitting to the Fano line shape. with various $|q|$'s.

We found that the lineshapes in the conductance $G_{tot}(V_g)$ can be well fitted to $G_{tot}(V_g) = G_{bg} + G_{Fano}(V_g)$. G_{Fano} is the Fano contribution expressed as

$$G_{Fano}(V_g) = A\frac{(\epsilon+q)^2}{1+\epsilon^2}, \quad \epsilon = \frac{\alpha(V_g - V_0)}{\Gamma/2}. \qquad (2)$$

A, V_0 and Γ are the strength, the position, and the width of the Fano resonance, respectively. α is the proportionality factor which relates V_g to the electrochemical potential of the QD. In our system, $\alpha \sim 20$ μeV/mV. G_{bg} is the constant background which represents the contribution of the electron transport through the upper arm with no interference. Typical results of the fitting are shown in Fig. 3 (b). Here, $|q| = 0.2$–7 and $\Gamma \sim 60$ μeV. The satisfying agreement means that the Fano state, namely the coherent mixture of the discrete state and the continuum, is formed over this QD-AB-ring system. The dip structure, which corresponds to $|q| < 1$, indicates a strong destructive interference, supporting that the electron passing the QD retains sufficient coherency to interfere with the one passing the arm in spite of the significant charging effect inside and around the QD.

The transport at finite source-drain bias (V_{sd}) also reveals the peculiar feature of this effect. Figure 4 shows the differential conductance at the lowest temperature as a function V_{sd} and V_g. The resonating conductance peak (white colored region) stretches along the line of $V_{sd} = 0$ μV with the Coulomb diamond superimposed. The observed width is consistent with Γ. The appearance of the zero-bias conductance peak even in the CB region indicates that the transmission through the QD is now allowed due to the aid of the continuum in the opposite arm. Such delocalization of the electron in the CB region is highly analogous with that observed in the QD in the Kondo regime [21] although the mechanism is different. Delocalization in the Kondo dot occurs through resonating spin singlet formation between the QD and the leads, while the Fano effect is supported by the resonance due to the configuration interaction between the discrete state and the continuum. And, as

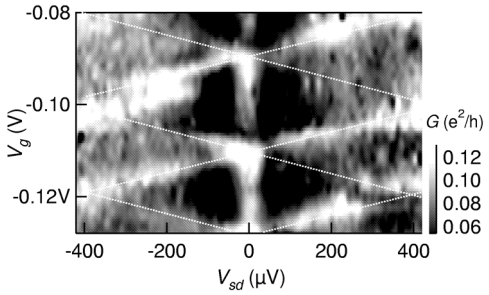

Fig. 4. Differential conductance obtained as a function of V_g at $T = 30$ mK and $B = 0.92$ T. The zero-bias conductance peak exists in the CB region with a Coulomb diamond superimposed. The edge of the CB region is emphasized with white dashed lines.

shown in Fig. 4, the Fano effect disappears at $|V_{sd}| \gg \Gamma/2$, meaning that the finite bias voltage quenches the Fano state by bringing strong quantum decoherence into the system.

The essential role of the coherence for the Fano effect is also confirmed by its temperature dependence. Figure 5 shows the conductance of the system between 50 mK and 800 mK. While clear Fano features appear at 50 mK as marked by the arrows, they diminish rapidly as the temperature increases. Especially, the asymmetric dips at 50 mK evolves into peaks at $T \geq 300$ mK. Although the thermal broadening of the Fano lineshape is not negligible at temperatures higher than Γ [19], it cannot explain such drastic temperature dependence. The main cause for this phenomenon is decoherence induced by increasing the temperature, resulting in the destruction of the Fano state. Then, asymmetric Fano line shapes gradually evolved into a Lorentzian line shape corresponding to $|q| \to \infty$, which indicates that the system is simply a classical parallel circuit of the QD and the arm.

3.2. *Phase Control of the Fano Interference*

The present system is mesoscopic in size, which is in clear contrast with the essentially microscopic nature of the other Fano systems. As we have already seen, the non-equilibrium Fano effect and the temperature dependence reveal the essence of the Fano effect. Above all, the largest advantage of the present system lies in the spatial separation between the discrete level and the continuum, which allows us to control Fano interference via the magnetic field piercing the ring. In Fig. 6 shows the 3D image plot of the conductance of the system as a function of V_g and B. Fano's asymmetric Coulomb oscillation appears in sweeping V_g at a fixed magnetic field, while the field sweeping at a fixed V_g results in the AB oscillation. The observed period of the AB oscillation is ~ 3.6 mT which is in agreement with the expected value for the ring size. The AB amplitude is found to be comparable to the Fano peak height. Again, this indicates that the electronic states form the coherent Fano state. Because the controlling of the phase and number of electrons yields the result in Fig. 6, it is legitimate to state that the wave-particle duality in the QD-AB-ring system results in the Fano effect.

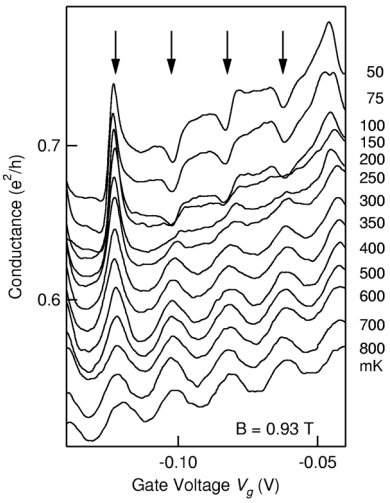

Fig. 5. Conductance of the system measured between 50 mK and 800 mK at $B = 0.93$ T. The data at $T < 700$ mK are incrementally shifted upward for clarity. The Fano features marked by the arrows at 50 mK gradually disappear as the temperature increases.

Figure 7(a) shows the conductance of one Fano peak at 30 mK at several magnetic fields. The direction of the asymmetric tail changes, for example, between $B = 0.9216$ T and 0.9232 T, while a symmetric shape appears in between at 0.9224 T. This result is sufficient for one to cast doubts on the applicability of Eq. (2) with a real q, because Eq. (2) never gives a symmetric lineshape for a real q unless $|q| \to \infty$ or $q = 0$ and the divergence of q should be ruled out.

To overcome the unphysical situation, we should take it into account that the field only affects the phase

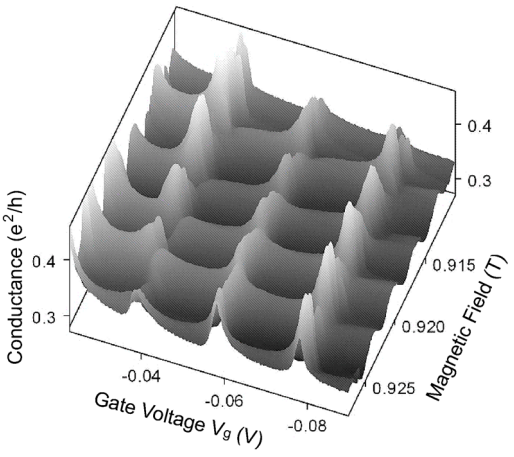

Fig. 6. Conductance of the three Fano peaks as a function of V_g and B at 30 mK.

of the electron and never changes the strength of the configuration interaction. As a consequence, the generalized Fano formula is proposed in the following expression as an expansion of Eq. (2),

$$G_{Fano} = A\frac{|\epsilon + q|^2}{\epsilon^2 + 1} = A\frac{(\epsilon + \mathrm{Re}q)^2 + (\mathrm{Im}q)^2}{\epsilon^2 + 1}. \quad (3)$$

This yields asymmetric and symmetric lineshapes for $\mathrm{Re}q \gg \mathrm{Im}q$ and $\mathrm{Re}q \ll \mathrm{Im}q$, respectively. Thus far we have treated q as real in the analysis of the Fano peaks, which is justified as their asymmetry is large enough.

It is noted that q has been implicitly treated as a real number in the original Fano theory [10]. This is valid only when the system has the time-reversal symmetry and thus the matrix elements defining q can be taken as real. The claim that Fano's asymmetric parameter q should be complex was theoretically considered in spectroscopy [22] and in the electron transport [6–9,23–25]. Within our knowledge, though, our result is the first convincing experimental indication that q should be a complex number.

We actually obtained the complex q by the numerical fitting. We used Eqn. 3 in $G_{tot} = G_{bg} + G_{Fano}$ and fitted each conductance curve at different B. The procedure was successful as shown in Fig. 7 (a) with solid curves. The obtained $\mathrm{Re}q$ and $\mathrm{Im}q$ are plotted in Fig. 7 (b). Both of them well depend on B sinusoidally, where the phase difference between the two sinusoids is $\pi/2$. The solid curves superposed on them are the result of fitting to the sinusoidal function.

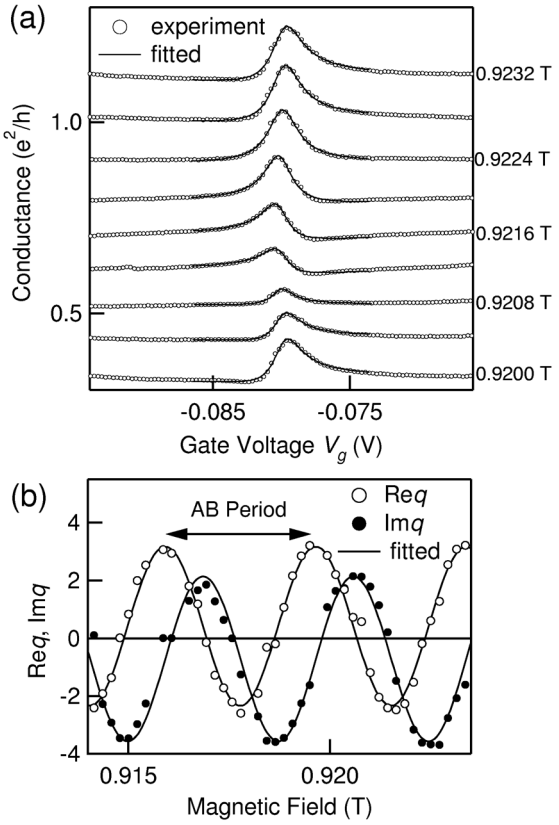

Fig. 7. (a) Conductance of the system measured at 30 mK at different magnetic fields. The open circles and the solid curves are the experiments and the results of the fitting, respectively. They are incrementally shifted upwards for clarity. (b) Obtained $\mathrm{Re}q$ and $\mathrm{Im}q$ are plotted. The solid curves are the fitted sinusoidal curves.

The conductance of the Fano system was theoretically proposed for the two-terminal setup [7,9]. The observed sinusoidal behavior of the $\mathrm{Re}q$ and $\mathrm{Im}q$ with the mutual phase difference of $\pi/2$ is consistent with the theory. The center of the oscillation is slightly shifted from zero in both $\mathrm{Re}q$ and $\mathrm{Im}q$ in the experiment as shown in Fig. 7 (b), while the theory predicts that both $\mathrm{Re}q$ and $\mathrm{Im}q$ oscillate symmetrically across zero. The difference might be due to the effect that is not included in the theoretical model. For example, the multi-channel transport and/or the finite incoherent transport through the system [24] may be responsible for the difference.

4. Conclusion

We report a tuning experiment of the Fano effect in the QD-AB-ring hybrid system. Delocalization of the discrete levels in the QD due to this effect shows up in the zero-bias peak in the differential conductance at finite V_{sd} and the considerable AB amplitude in the CB region. Through the magnetic controlling of the Fano line shape, we found that the Fano parameter q should be a complex number. By the numerical fitting, complex q was obtained as a sinusoidal function of B.

It is interesting to note that the Fano effect first established in atomic physics is now observed in an artificial atom system. Such a mesoscopic analog will bring us renewed understanding for this familiar effect. For example, the complex q that we derive here will be also investigated in other experiments where the time-reversal symmetry is broken.

ACKNOWLEDGMENTS

We thank A. Aharony, M. Büttiker, O. Entin-Wohlman, M. Eto, W. Hofstetter, T.-S. Kim, J. König, and T. Nakanishi for helpful discussion. This work is supported by a Grant-in-Aid for Scientific Research and by a Grant-in-Aid for COE Research ("Quantum Dot and Its Application") from the Ministry of Education, Culture, Sports, Science, and Technology of Japan. K.K. is supported by a Grant-in-Aid for Young Scientists (B) (No. 14740186) from Japan Society for the Promotion of Science.

References

[1] A. Yacoby, M. Heiblum, D. Mahalu, and H. Shtrikman, Phys. Rev. Lett. **74,** 4047 (1995).

[2] R. Schuster, E. Buks, M. Heiblum, D. Mahalu, V. Umansky, and H. Shtrikman, Nature **385,** 417 (1997).

[3] P. Singha Deo and A. M. Jayannavar, Mod. Phys. Lett. B **10,** 787 (1996); P. Singha Deo Solid St. Commun. **107,** 69 (1998).

[4] C.-M. Ryu and S. Y. Cho, Phys. Rev. B **58,** 3572 (1998).

[5] K. Kang, Phys. Rev. B **59,** 4608 (1999).

[6] O. Entin-Wohlman, A. Aharony, A., Y. Imry, and Y. Levinson, J. Low Temp. Phys. **126,** 1251 (2002).

[7] W. Hofstetter, J. König, and H. Schoeller, Phys. Rev. Lett. **87,** 156803 (2001).

[8] Tae-Suk Kim, Sam Young Cho, Chul Koo Kim, and Chang-Mo Ryu: Phys. Rev. B **65,** 245307 (2002).

[9] A. Ueda, I. Baba, K. Suzuki, and M. Eto, J. Phys. Soc. Jpn. **72,** Suppl. A, 157 (2003).

[10] U. Fano, Phys. Rev. **124,** 1866 (1961).

[11] U. Fano and A. R. P. Rau, *Atomic Collisions and Spectra* (Academic Press, Orland , 1986).

[12] F. Cerdeira, T. A. Fjeldly, and M. Cardona, Phys. Rev. B **8,** 4734 (1973).

[13] J. Faist, F. Capasso, C. Sirtori, K. W. West, and L. N. Pfeiffer, Nature **390,** 589 (1997).

[14] E. Tekman and P. F. Bagwell, Phys. Rev. B **48,** 2553 (1993).

[15] J. U. Nöckel and A. D. Stone, Phys. Rev. B **50,** 17415 (1994).

[16] V. Madhavan, W. Chen, T. Jamneala, M. F. Crommie and N. S. Wingreen, Science **280,** 567 (1998).

[17] J. Li, W. D. Schneider, R. Berndt, and B. Delley, Phys. Rev. Lett. **80,** 2893 (1998).

[18] J. Göres, D. Goldhaber-Gordon, S. Heemeyer, M. A. Kastner, H. Shtrikman, D. Mahalu, and U. Meirav, Phys. Rev. B **62,** 2188 (2000).

[19] I. G. Zacharia, D. Goldhaber-Gordon, G. Granger, M. A. Kastner, Yu. B. Khavin, H. Shtrikman, D. Mahalu, and U. Meirav, Phys. Rev. B **64,** 155311 (2001).

[20] K. Kobayashi, H. Aikawa, S. Katsumoto, and Y. Iye, Phys. Rev. Lett. **88,** 256806 (2002).

[21] D. Goldhaber-Gordon, H. Shtrikman, D. Mahalu, D. Abusch-Magder, U. Meirav and M.A. Kastner: Nature **391,** 156 (1998); S. M. Cronenwett, T. H. Oosterkamp, and L. P. Kouwenhoven, Science **281,** 540 (1998); J. Schmid, J. Weis, K. Eberl, and K. von Klitzing, Physica B **256-258,** 182 (1998).

[22] G. S. Agarwal, S. L. Haan, and J. Cooper, Phys. Rev. A **29,** 2552 (1984); G. Abstreiter, M. Cardona, and A. Pinczuk, in *Light Scattering in Solids*, edited by M. Cardona and G. Güntherodt, Topics in Applied Physics Vol. 54 (Springer, Berlin, 1984), p. 127; K. J. Jin, S. H. Pan, and G. Z. Yang, Phys. Rev. B **50,** 8584 (1994); Wolfgang Ihra, Phys. Rev. A **66,** 020701 (2002).

[23] E. R. Racec and Ulrich Wulf, Phys. Rev. B **64,** 115318 (2001).

[24] A. A. Clerk, X. Waintal, and P. W. Brouwer Phys. Rev. Lett. **86,** 4636 (2001).

[25] K. Kang and S.-Y. Cho, cond-mat/0210009.